Mechanism Diversity of the Loma Prieta Aftershocks and the Mechanics of Mainshock-Aftershock Interaction

Gregory C. Beroza and Mark D. Zoback

The diverse aftershock sequence of the 1989 Loma Prieta earthquake is inconsistent with conventional models of mainshock-aftershock interaction because the aftershocks do not accommodate mainshock-induced stress changes. Instead, the sense of slip of the aftershocks is consistent with failure in response to a nearly uniaxial stress field in which the maximum principal stress acts almost normal to the mainshock fault plane. This orientation implies that (i) stress drop in the mainshock was nearly complete, (ii) mainshock-induced decreases of fault strength helped were important in controlling the occurrence of aftershocks, and (iii) mainshock rupture was limited to those sections of the fault with preexisting shear stress available to drive fault slip.

Because they are aftershocks, relatively small earthquakes that occur in and adjacent to the rupture zone of a large earthquake are related to the mainshock that brought them about. Two heuristic models of mainshock-aftershock interaction that relate the location and sense of slip of aftershocks to those of the mainshock are the barrier and asperity models (*1*) (Fig. 1). In the barrier model, the shear stress that acts in the plane of a fault before the mainshock is relatively uniform, but the fault strength is spatially variable. During an earthquake, slip occurs on weaker parts of the fault but does not propagate through relatively high-strength barriers. Shear stress along the fault decreases where slip occurs but increases in the unbroken barriers. Aftershocks represent the eventual failure of these barriers in response to the stress increase imposed by the mainshock. In the asperity model, the shear stress before the mainshock is spatially variable and the highly stressed asperities break in the mainshock. Aftershocks occur in response to stress transfer from the asperity to surrounding regions. In both models, aftershocks occur in response to a static stress change: either an increase in shear stress or a decrease in normal stress that results from the mainshock.

A number of investigators have shown that aftershocks surround areas of high slip in mainshocks (*2*) (Figs. 1 and 2). This observation is consistent with both the barrier and asperity models. To perform a more rigorous test of these models and to investigate the causal relation between a large earthquake and its aftershocks, we studied the 1989 Loma Prieta, California, mainshock and its aftershock sequence. Because the Loma Prieta earthquake occurred in a densely instrumented region, detailed knowledge of the slip in the mainshock and of the locations and focal mechanisms of the aftershocks is unprecedented. If stress changes induced by the mainshock cause aftershocks, then the aftershocks should occur either in areas where the mainshock increases shear stress or decreases normal stress.

The Loma Prieta mainshock occurred in the southern Santa Cruz Mountains on a southwest-dipping plane (*3*). The P-wave polarities (*4*), long-period teleseismic data (*5*), and geodetic data (*6*) all indicate that the overall sense of slip was oblique, with components of both right-lateral and reverse slip. A surprising aspect of the Loma Prieta aftershock sequence was that many aftershocks that occurred near the mainshock fault plane showed diverse mechanisms (*4, 7, 8*). There were large numbers of right-lateral, left-lateral, reverse, and normal faulting aftershocks (Fig. 2). This diversity persists even when only aftershocks with nodal planes subparallel to the mainshock fault plane are considered. Several investigators (*4, 8*) suggested that a heterogeneous post-mainshock stress field was the most probable explanation for the various mechanisms. An important aspect of the diversity is that it occurred both in areas that ruptured during the mainshock and in adjacent areas that did not (Fig. 2). In many locations, seemingly incompatible types of earthquakes (that is, right- and left-lateral or reverse and normal) occurred in approximately the same place. For example, in a limited area about 15 km northwest of the hypocenter at depths of 12 to 16 km, aftershocks with all four types of mechanisms were observed. In terms of conventional faulting theory, this diversity is possible only if the fault zone is extremely weak (*9*). More puzzling, the diversity of the aftershock mechanisms was inconsistent with mainshock-induced stress changes. That is, because slip in the mainshock was right-lateral and reverse, aftershocks in the mainshock fault plane that surrounded the slipped zone should also have been right-lateral and reverse. However, numerous left-lateral and normal aftershocks (Fig. 2) were observed (*10*).

The abundant on-scale, near-source records of ground motion for the Loma Prieta mainshock made it possible to infer the spatial variation of slip and several models of the slip distribution that are based on these data are available (*11–13*). We adopt-

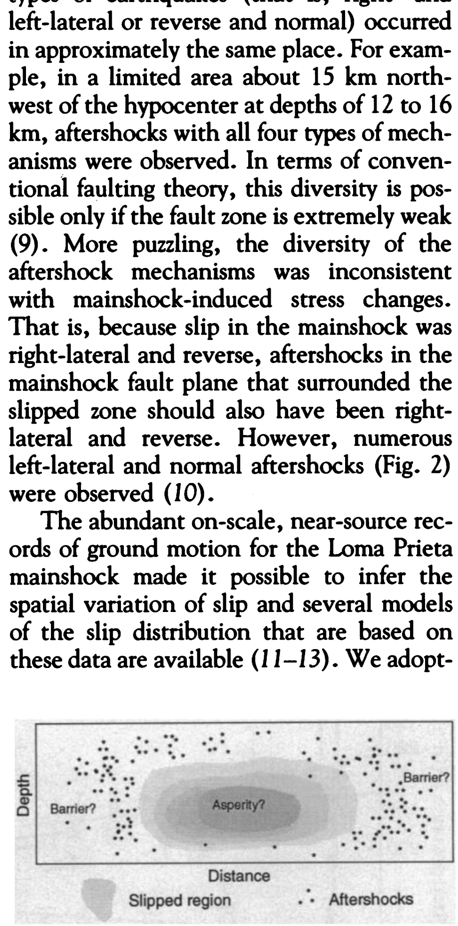

Fig. 1. Schematic representation of aftershocks that surround areas of high slip (*2*) in terms of two models of inhomogeneous faulting and aftershocks. Parts of the fault that undergo large changes in the static stress field are the areas of high aftershock activity. In the barrier model, slip in the mainshock occurs on weak parts of the fault bounded by barriers and aftershocks represent the eventual failure of the high-strength barriers. In the asperity model aftershocks occur around the strong asperity. A fundamental assumption in both models is that aftershocks occur in response to mainshock-induced changes in shear and normal stress.

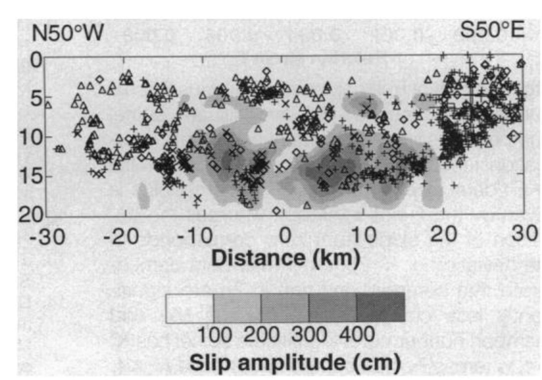

Fig. 2. The total slip amplitude for the Loma Prieta earthquakes in side view, with 979 well-located aftershocks that had well-constrained focal mechanisms. Depth is in kilometers. The aftershocks are plotted by mechanism: (+) right lateral, (×) left lateral, (△) reverse, and (◇) normal. Mechanism is defined by the use of the aftershock nodal plane most nearly parallel to the mainshock fault plane.

Department of Geophysics, Stanford University, Stanford, CA 94305–2215.

Table 1. Sign of interpretation of **M**:Δ**T**; MIS, mainshock-induced shear.

	M:Δ**T** > 0	**M**:Δ**T** < 0
Δ**T** > 0	Consistent with MIS	Inconsistent with MIS
Δ**T** < 0	Complete dynamic overshoot	Delayed mainshock rupture

ed the rupture model of Beroza (*11*) (Fig. 2) to interpret the aftershocks. In this model, most of the coseismic slip occurred in two regions on either side of the mainshock hypocenter; slip was primarily right-lateral to the southeast and primarily reverse to the northwest. Although some important differences exist between different slip models of the Loma Prieta earthquake (*11–13*), the spatial extent, amplitude, and direction of slip are similar (*14*).

We calculated the mainshock-induced stress change, ΔT, from the slip distribution shown in Fig. 2 (*15*). The stress change over most of the mainshock fault plane is on the order of 5 MPa (*16*), with peak values of 10 to 40 MPa. We calculated the stress change at each aftershock hypocenter and used this value to determine the traction change on the aftershock plane induced by the mainshock. We then calculated the projection of the traction change vector onto the slip vector to test whether this change could have induced slip in the observed direction. The aftershock relieves mainshock-induced shear stress only if there is a component of slip in the same direction as the traction change. To test this condition, we evaluated the sign of the tensor dot product, **M**:Δ**T**, between the aftershock moment tensor **M** and the stress-change tensor Δ**T** (*17*). The interpretation of **M**:Δ**T** depends on the sign of the stress change (Table 1).

To visualize the four cases in Table 1, consider the result of right-lateral slip on the mainshock fault plane. For aftershocks that occur on this plane, only right-lateral aftershocks in the region of right-lateral traction increase that surrounds the slipped patch are consistent with mainshock-induced shear (Δ**T** > 0 and **M**:Δ**T** > 0). On the other hand, if a right-lateral aftershock occurs in a region where slip took place and caused the right-lateral traction to decrease (Δ**T** < 0 and **M**:Δ**T** < 0), then the aftershock must represent delayed rupture of the fault, which implies that the mainshock weakened the fault plane. If a left-lateral aftershock occurs in a region that slipped and right-lateral stress decreased (Δ**T** < 0 and **M**:Δ**T** > 0), then the aftershock implies a complete reversal of the shear stress acting on the fault plane (that is, complete dynamic overshoot). Finally, if a left-lateral aftershock occurs in a region of right-lateral traction increase (Δ**T** > 0 and **M**:Δ**T** < 0), then the mainshock could not have caused the aftershock, at least through a change in shear stress.

Only about half (52%) of the aftershocks of the Loma Prieta earthquake relieved the mainshock-induced stress changes (Fig. 3), which is essentially no better than the 50% expected from a random population of aftershock mechanisms (*18*). More problematic, many of the aftershocks require complete dynamic overshoot (*10*) and the many normal and left-lateral mechanisms remain unexplained. The precise values of the traction changes vary with gradients of the slip distribution (which are not well constrained). However, the results shown in Fig. 3 depend primarily on the orientation and spatial extent of the net stress change in the plane of the fault, which in turn depends primarily on where slip occurred in the mainshock. Significantly different results would not have been obtained had another slip model been used (*19*).

A decrease in normal stress could be just as effective as an increase in shear stress in the initiation of failure. We tested the hypothesis that the Loma Prieta aftershocks were induced by decreases in normal stress that resulted from mainshock slip. The expressions Δ**T:nn** and Δ**T:ss** represent the tensor dot products of the stress change tensor with the outer products, **nn** and **ss**, of the two possible aftershock fault-normal vectors. If the sign of either of these tensor products is positive, then a normal stress change could have facilitated failure in the aftershock. In this case, 75% of a random assemblage of aftershocks should satisfy this criterion for one of the two possible normal vectors. Because one of these quantities is positive for only ~67% of the aftershocks, a decrease in normal stress cannot explain the aftershock mechanisms.

The mainshock-induced stress changes clearly do not account for the diversity of aftershock mechanisms. Therefore, we sought an alternative model in which the aftershock mechanisms could be explained by a uniaxial normal stress that acts across the mainshock fault plane (*20*). By investigating this case we can test two hypotheses at once. For aftershocks that occurred in the region of mainshock slip, we are investigating the hypothesis of complete stress drop. Complete stress drop is consistent with the idea that the San Andreas fault is weak and moves at extremely low levels of shear stress (*21*). For aftershocks on parts of the fault that did not slip in the mainshock, consistency between the sense of slip in the aftershocks and a uniaxial stress field implies that rupture did not occur in these areas during the mainshock because shear stress was absent.

If $\mathbf{T}_n$ represents a uniaxial, fault-normal stress field, then aftershocks for which $\mathbf{M}:\mathbf{T}_n > 0$ are consistent with the uniaxial fault-normal compression hypothesis and aftershocks for which $\mathbf{M}:\mathbf{T}_n < 0$ are inconsistent with it (Fig. 4). Comparison of Fig. 4A with Fig. 3A shows that the percent of mechanisms consistent with fault-normal compression (75%, including most of the left-lateral and normal events) is significantly greater than that consistent with mainshock-induced shear (52%). Thus, it is possible to explain most of the mechanism diversity with a simple, uniform fault-normal compressive stress.

We performed a more rigorous test of the consistency of the aftershock data with a uniform post-mainshock stress field by inverting the aftershock mechanisms to obtain the best-fitting stress tensor (*21*). The method we used to determine the stress

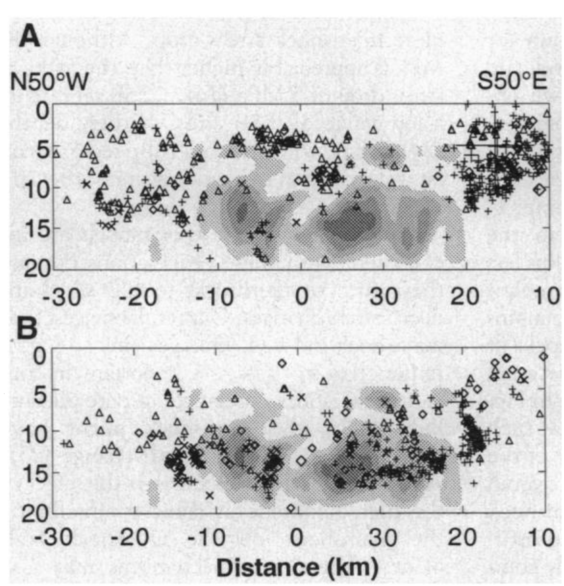

Fig. 3. Aftershocks plotted by mechanism for (**A**) those events that relieve the mainshock stress change and (**B**) those that do not. Only 52% of the aftershocks relieve mainshock-induced stress change. Mechanisms and slip amplitude indicated as in Fig. 2.

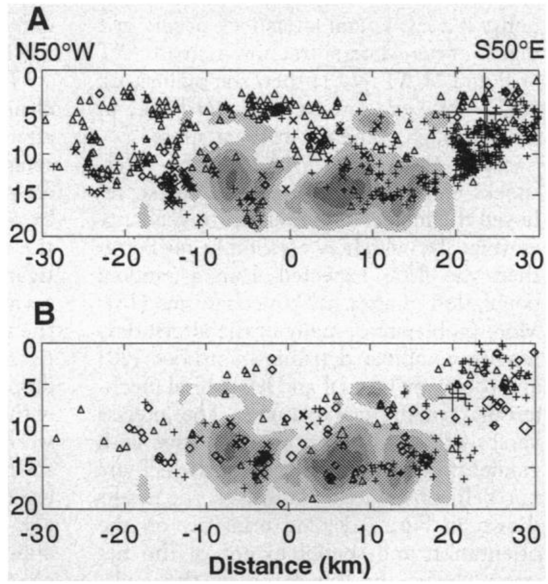

Fig. 4. (**A** and **B**) As in Fig. 2 but for a stress field of pure fault-normal compression. This model explains 75% of the aftershocks.

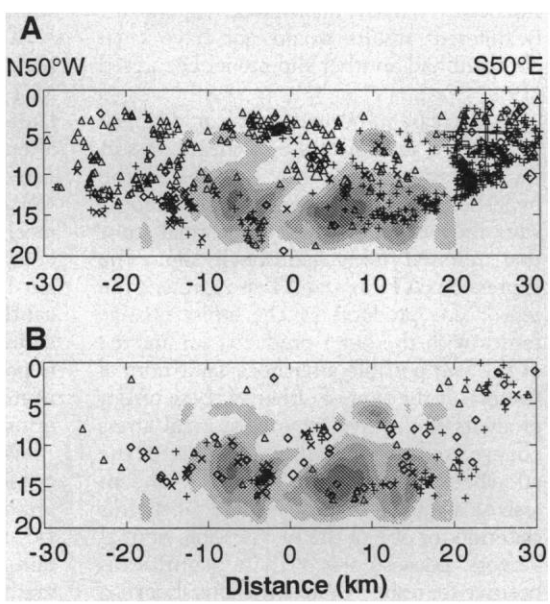

Fig. 5. (**A** and **B**) As in Fig. 2 but for the best-fitting uniform stress field. This model explains 84% of the aftershocks, and the average misfit is only 11°.

tensor from focal mechanisms allows for errors in both the fault planes and slip directions (*22*). The stress tensor we obtained has a maximum principal compressive stress that strikes N27°E and plunges 12°, and the intermediate stress axes are nearly equal (*23*). The maximum compressive stress is rotated by ~13° from the mainshock fault-normal vector and dips less steeply, which suggests that a small amount of residual shear stress remains on the mainshock fault plane; 84% of the aftershocks fit this model (Fig. 5A). The contrast between the results shown in Fig. 3 and those in Fig. 5 is profound, and it is surprising that such a simple model can explain so many of the diverse mechanisms. Because of an overall lack of shear stress on the post-mainshock fault plane, the 10- to 40-MPa stress drop in the high-slip regions represents nearly complete mainshock stress drop. Although 40 MPa is appreciably higher than the average stress drop of 5 MPa (*16*), it still represents a low value of shear stress at these depths (*24*). Thus, while the high-slip regions may be stronger than surrounding areas, they are still weak in an absolute sense.

The asperity and barrier models are inconsistent with these observations because they attribute aftershocks to mainshock-induced stress changes. Our results suggest that mainshock-induced changes in strength, rather than in stress, are important in triggering aftershocks. Changes in pore pressure induced by the mainshock might have caused this apparent strength change (*25*). Another possible mechanism is the effect of the high-amplitude dynamic strains during the mainshock on the aftershock fault planes. These two mechanisms may also explain the observed spatial distribution of aftershocks with respect to regions of high mainshock slip (*2*).

The origin of aftershocks as a response to a uniform stress tensor that followed complete stress drop is more consistent with the asperity model (smooth post-seismic stress field) than with the barrier model (heterogeneous post-seismic stress field). Moreover, our observations are consistent for aftershocks that occurred both inside and outside of the mainshock rupture zone. Thus, slip in the mainshock may have been limited to only those sections of the fault in which there was preexisting shear stress to drive fault slip, an observation that is also generally consistent with the asperity model.

In addition to their suggestions of complete stress drop, earlier investigators speculated that small-scale block rotations or complexities introduced by nonplanar faulting might explain the diverse aftershocks of the Loma Prieta sequence (*4*, *8*). Complexities of the slip pattern and stress redistribution in the mainshock may help to explain some of this diversity. However, a much more simple model in which mainshock stress drop was near complete, slip in the aftershocks was driven by the residual fault-normal compression (*26*), and mainshock-induced strength changes helped trigger aftershocks explains the data more completely.

REFERENCES AND NOTES

1. S. Das and K. Aki, *J. Geophys. Res.* **82**, 5658 (1977); H. Kanamori and G. Stewart, *ibid.* **83**, 3427 (1978).
2. R. S. Stein and M. Lisowski, *ibid.* **88**, 6477 (1983); C. Mendoza and S. H. Hartzell, *Bull. Seismol. Soc. Am.* **78**, 1438 (1988); G. C. Beroza and P. Spudich, *J. Geophys. Res.* **93**, 6275 (1988); H. Houston and E. R. Engdahl, *Geophys. Res. Lett.* **16**, 1421 (1989); S. Y. Schwartz, J. W. Dewey, T. Lay, *J. Geophys. Res.* **94**, 5637 (1989).
3. For a summary of the Loma Prieta earthquake and its effects, see U.S. Geological Survey Staff, *Science* **247**, 286 (1990).
4. D. H. Oppenheimer, *Geophys. Res. Lett.* **17**, 1199 (1990).
5. J. Zhang and T. Lay, *ibid.*, p. 1195.
6. M. Lisowski, W. H. Prescott, J. C. Savage, M. J. Johnston, *ibid.*, p. 1437.
7. We limited our analysis to aftershocks that occurred within 21 months of the mainshock, were within 30 km of the hypocenter along strike, and within 10 km of the dipping fault plane. Only aftershocks with 90% confidence levels of less than 30° about the estimated values for strike, dip, and rake were used. We characterized aftershocks by type using the rake associated with the aftershock nodal plane closest to the mainshock fault plane.
8. A. J. Michael, W. L. Ellsworth, D. H. Oppenheimer, *Geophys. Res. Lett.* **17**, 1441 (1990).
9. The proximity of aftershocks with seemingly inconsistent mechanisms, such as reverse and normal events, requires faulting on weak planes because the maximum and minimum principal stresses must be exchanged. Assumption of laboratory-derived coefficients of friction of 0.6 to 1.0 and hydrostatic pore pressure would require stress changes of hundreds of megapascals over distances of only a few kilometers at seismogenic depths [R. H. Sibson, *Nature* **249**, 542 (1974)].

10. Left-lateral and normal aftershocks on planes subparallel to the mainshock could conceivably occur where the fault slipped but only if there was complete dynamic overshoot (a complete reversal of shear stress on the fault plane as a result of the mainshock slip). This behavior is extremely unlikely. Theoretical rupture calculations indicate that dynamic overshoot is a small effect, with a value at most of ~15% of the difference between the static and dynamic friction levels [for example, R. Burridge and G. S. Halliday, *Geophys. J. R. Astron. Soc.* **25**, 261 (1971)]. For dynamic overshoot to explain left-lateral and normal aftershocks in the regions of right-lateral and reverse stress drop certain conditions would be required. The dynamic frictional strength of the fault would have to be nearly zero, and the overshoot would have to be so extreme as to change completely the sign of stress on the fault and cause failure in the opposite direction in the aftershock.
11. G. C. Beroza, *Bull. Seismol. Soc. Am.* 81, 1603 (1991).
12. J. H. Steidl, R. J. Archuleta, S. H. Hartzell, *ibid.*, p. 1573.
13. D. J. Wald, D. V. Helmberger, T. H. Heaton, *ibid.*, p. 1540.
14. There is an inherent nonuniqueness in the inference of fault slip from seismic observations because the problem is underdetermined. Regularization techniques give solutions subject to a priori constraints such as smoothness. See A. H. Olson and J. G. Anderson, *Geophys. J.* **94**, 443 (1988).
15. We calculated ΔT using the rupture model (*7*) in a general program [L. Ericksen, thesis, Stanford University (1986)] for calculating stresses in an elastic half space due to rectangular dislocation sources. We have approximated the spatially varying slip model with 8554 dislocations.
16. H. Kanamori and K. Satake, *Geophys. Res. Lett.* 17, 1179 (1990).
17. There is an ambiguity when one discriminates the aftershock fault plane from the auxiliary plane. However, because of the symmetry of the stress tensor and moment tensors, the projection of the mainshock-induced traction onto the slip vector is the same for both possible fault planes. This quantity may be calculated from the stress change $\Delta\mathbf{T}$ and the aftershock moment tensor $\mathbf{M}$. The normalized

$$\mathbf{M} = 1/2(\mathbf{ns} + \mathbf{sn})$$

and

$$1/2\mathbf{M}{:}\Delta\mathbf{T} = \mathbf{s} \cdot \Delta\mathbf{T} \cdot \mathbf{n} = \mathbf{n} \cdot \Delta\mathbf{T} \cdot \mathbf{s}$$

but these last two expressions are simply the projection of the slip vectors onto the mainshock traction change. This quantity has been used to study variations in the stress field after the 1987 Whittier Narrows earthquake [A. J. Michael, *J. Geophys. Res.* **96**, 6303 (1991)]. We define a spatially variable stress change (stress drop) to determine the sign of ΔT using displacements and traction changes determined from the elastostatic solution. If the stress decreased, then $\Delta\mathbf{T}\cdot\mathbf{u} < 0$ and, if the stress increased, then $\Delta\mathbf{T}\cdot\mathbf{u} > 0$. Left-lateral and normal aftershocks for which $\Delta\mathbf{T} < 0$ and $\mathbf{M}{:}\Delta\mathbf{T} > 0$ would imply that there was complete dynamic overshoot.
18. The inner product of two vectors, in this case traction and slip vectors, will be positive 50% of the time if their orientation is random.
19. Because slip in the Loma Prieta mainshock was a combination of right-lateral and reverse on a dipping plane, it is incapable of explaining the unexpected left-lateral and normal mechanisms on subparallel planes. Moreover, no slip model can explain incompatible pairs of events in the same area, especially regions far from the mainshock. That is, an earthquake cannot cause stress to change in two directions at once. If slip occurred over a larger area than in the model (*7*), even more left-lateral and normal aftershocks would have occurred in regions of stress drop and would require that there was complete dynamic overshoot. If slip occurred over a smaller area than in the model, the aftershocks that occurred far from the hypocenter are even more difficult to understand.
20. M. D. Zoback and G. C. Beroza, *Geology*, in press.
21. The extremely low strength of the San Andreas fault is indicated by the absence of a frictionally generated heat-flow anomaly [J. N. Brune, T. L. Henyey, R. Roy, *J. Geophys. Res.* **74**, 3821 (1969); see also A. H. Lachenbruch, *ibid.* **85**, 6097 (1980)]. Observations in central California also show that the direction of maximum principal stress is nearly perpendicular to the San Andreas fault, so that there is little resolved shear stress on it [M. D. Zoback *et al.*, *Science* **238**, 1105 (1987); V. S. Mount and J. Suppe, *Geology* **15**, 1143 (1987)].
22. J. W. Gephart and D. W. Forsyth, *J. Geophys. Res.* **89**, 9305 (1984). We find that the quantity $(S_1 - S_3)/(S_2 - S_3) = 0.7$, which indicates that the intermediate and minimum principal stresses, S_2 and S_3, are comparable.
23. The average residual of ~11° and the generally small residuals over the entire aftershock zone indicate that a predominantly uniform stress tensor of near fault-normal compression is consistent with the observed aftershock diversity.
24. R. H. Sibson, in (*9*).
25. A. Nur and J. R. Booker, *Science* **175**, 885 (1972); A. H. Lachenbruch, in (*21*).
26. Aftershocks of the 1984 Morgan Hill (magnitude = 6.1) earthquake were analyzed with a similar technique [D. H. Oppenheimer, P. A. Reasenberg, R. W. Simpson, *J. Geophys. Res.* **93**, 9007 (1988)]. Unlike the Loma Prieta earthquake, the Morgan Hill event had aftershocks that occurred on the mainshock fault plane had the same right-lateral mechanism as the mainshock. However, the off-fault seismicity did show evidence of fault-normal compression and was cited as evidence that the Calaveras fault is weak.

27. We thank D. Oppenheimer for his fault-plane solutions and B. Ellsworth, A. Michael, P. Segall, and R. Simpson for helpful discussions. Supported by a National Science Foundation Presidential Young Investigator Award (G.B.), a Shell Faculty Career Initiation Grant (G.B.), and U.S. Geological Survey grant 14-08-0001-G1853 (M.Z.).

17 March 1992; accepted 15 October 1992

Domain Structures in Langmuir-Blodgett Films Investigated by Atomic Force Microscopy

L. F. Chi, M. Anders, H. Fuchs,* R. R. Johnston, H. Ringsdorf

Investigations of phase-separated Langmuir-Blodgett films by atomic force microscopy reveal that on a scale of 30 to 200 micrometers, these images resemble those observed by fluorescence microscopy. Fine structures (less than 1 micrometer) within the stearic acid domains were observed, which cannot be seen by conventional optical microscopic techniques. By applying the force modulation technique, it was found that the elastic properties of the domains in the liquid condensed phase and grains observed within the liquid expanded phase were comparable. Small soft residues in the domains could also be detected. The influence of trace amounts of a fluorescence dye on the micromorphology of monolayers could be detected on transferred films.

Langmuir-Blodgett (LB) and related thin organic films have been the objects of increasing technological and scientific interest over the past 20 years (*1–4*). Optimization of the macroscopic physical properties of these systems requires a detailed understanding of their structure-property relations on a microscopic scale, including the structure of transferred LB films on solid substrates, the nucleation of crystalline phases, and their phase transitions. At the air-water interface the phase states of lipid monolayers and their transitions, such as the formation of domains in the coexistence region of liquid condensed–liquid expanded (LC-LE) phases, have been investigated by fluorescence microscopy (*5–9*). Similar studies on transferred LB films at the air-substrate interface, however, have rarely been reported (*10*). Fluorescence microscopy is limited to structures larger than 1 μm in diameter. Electron microscopy has also been applied to image domain structures (*11, 12*). However, the imaging technique applied (phase contrast transmission

L. F. Chi, M. Anders, H. Fuchs, BASF AG, Polymer Research Laboratory, ZKM/T-J543, W-6700 Ludwigshafen, Germany.
R. R. Johnston and H. Ringsdorf, Institute of Organic Chemistry, Johannes Gutenberg University, J. J. Becherweg 18-20, W-6500 Mainz, Germany.

*To whom correspondence should be addressed.

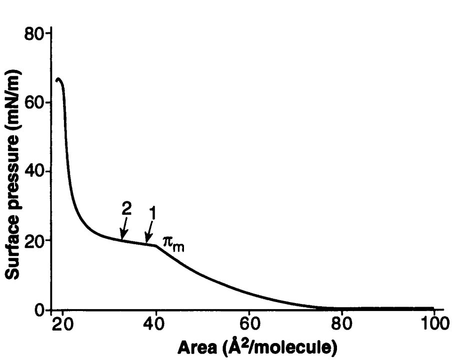

Fig. 1. Isotherm of surface pressure (π) versus area per molecule of stearic acid on a poly(ethyleneimine) (PEI, M_n = 1800)–containing aqueous subphase. The conditions are as follows: T = 20°C, V_c = 2.84 Å² molecule^{-1} min^{-1}. The pressure of the main phase transition (π_m, position 1) and different positions for film transfers are marked with arrows.